OPTICAL COMMUNICATIONS TERMINALS WITH PRECISE POINTING

Thomas E D Frame and Alexandre Pechev

Surrey Space Centre,

University of Surrey,

Guildford, GU2 7XH, UK

E-mail: T.Frame@surrey.ac.uk

ABSTRACT

Increasing data bandwidth requirements from spacecraft systems is beginning to pressure existing microwave communications systems. Free-Space optical communications allows for larger bandwidths for lower relative power consumption, smaller size and weight when compared to the microwave equivelant. However optical communication does has a formidable challenge that needs to be overcome before the advantages of the technology can be fully utilized. In order for the communication to be successful the transmitter and receiver terminals need to be pointed with a high accuracy (generally in the order of $\leq 10\mu$ radians) for the duration of communication. In this paper we present a new concept for precise pointing of optical communications terminals (termed the Precise Pointing Mechanism). In this new concept we combine the separate pointing mechanisms of a conventional optical terminal into a single mechanism with a targeted goal of less than 3μ radians pointing accuracy within a field of view of $10°$ by electromagnetically actuating the whole telescope assembly over 6 degrees-of-freedom. This paper discusses the principles of operation of this new terminal, the design and modeling of an engineering model using a combination of permanent magnets and reluctance force electromagnets to provide the actuation with the required pointing precision.

Key words: Optical Communications, Magnetic Levitation, Control, precise pointing.

1. INTRODUCTION

Communication is an ever growing and advancing field that is driven by many differing factors. As advances in space borne instrumentation and data gathering/processing systems advance, an inherent increase in the data rate and bandwidth of the communications system follows. Optical terminals can provide advantages in larger data bandwidths, lower relative power consumption, smaller size/weight over microwave systems due to the nature of the medium used [1]. However due to the narrow divergence of the medium used in optical communications a very accurate and responsive pointing system is required in order to maintain the link between the communication terminals. Generally optical terminals consist of a fixed Telescope acting as the antenna and a series of mirror assemblies (the Coarse Pointing Assembly (CPA), Fine Pointing Assembly (FPA) and the Point Ahead Assembly (PAA)). In an ESA initiative, the Small Optical User Terminal (SOUT) the CPA (which in this case consists of a pair of mirrors) is gimbaled using stepping motors together with gears to give a rotation in the elevation and azimuth directions [2]. In the ISLFE optical terminal the CPA mirror is gimbaled using a hybrid stepper motor to give azimuth and elevation direction [3]. The fine pointing mechanism generally consists of a pair of mirrors that work together to focus the beam onto the receiver unit. In the SOUT terminal the FPA uses a single mirror that is manipulated using a permanently excited DC motor [2]. In the ISLFE terminal however the FPA consists of a single mirror that is connected to Lorentz force actuators that manipulate it using capacitive sensors to control the angular position [3]. A major requirement of the pointing system is to overcome spacecraft disturbances and maintain the optical link for the duration of communication. From studies looking at spacecraft disturbances it can be seen that the bandwidth of the pointing mechanism needs to overcome a broad range of disturbances [4] [5] [6] [7]. Magnetic levitation technology provides a solution to the bandwidth requirement of the pointing mechanism, and offers infinite resolution that is only constrained by the sensor resolution and noise. In this research the separate pointing mechanisms are be combined into a single unit whose bandwidth fulfills the requirements of the separate mechanisms. Magnetic levitation has been considered and implemented in many areas and differing fields, and achieved high precision positioning, as demonstrated by [8] [12]. However this technology has not been applied to a space-borne magnetically levitated optical telescope. The system developed by [8] levitates a 6-DOF triangular platform that demonstrates a 5nm position resolution for 6 axis but has a very small travel range in the order of μmetres. Used effectively this technology can provide the accuracy require-

ments in order to maintain an effective optical communications link [8] [10] [9].

The purpose of this paper is to introduce how magnetic levitation technology will be applied to levitate and actuate the telescope element of an optical communications scenario through 6 degrees of freedom (DOF). An overview of the current Precise Pointing Mechanism (PPM) design, the dynamics and the control system are discussed.

2. THE PRECISE POINTING MECHANISM (PPM)

The concept proposed in this research differs from the traditional optical terminal system as the separate mirror assemblies will be combined into a single unit. Through the use of eight sets of electromagnets and four pairs of permanent magnets the entire telescope assembly will be levitated and manipulated through $\pm5°$. This reduces the number of components required in the optical bench and the number of mechanisms to manipulate the mirrors but increases the complexity of the control system and sensors required. The $10°$ field of view (FOV) does limit the application of this terminal as a stand alone device, but placement on a gimbal assembly to increase this FOV would allow for a wider range of mission scenarios. With the $10°$ FOV alone the main applications are to terrestrial communications terminals (such as inter-building communication links), Formation flying missions, rendezvous and docking or a GEO-LEO relay satellite in the micro-sat range. For this research the emphasis is on developing an engineering model of a receiver terminal in order to allow us to develop and validate the principle and controllers designed.

2.1. System Configuration

The pointing mechanism consists of eight custom designed electromagnets which are used to control the translation about X, Y and Z, and rotations about those axis (ϕ, ρ and ψ respectively as related to Fig 2). The optical elements used to form the telescope comprise of a 60 mm diameter primary mirror, and 24 mm diameter secondary mirror in a Schmidt-cassegrain configuration to produce an F-number of 5 (found to be the best suited design for telescope speed versus focus quality). The secondary mirror is held in place through a spider configuration mount that has been designed to have minimum effect on the optical image seen at the focal plane. The primary and secondary mirror have been designed according to a link analysis undertaken during the optical design. The theoretical receiver power curve produced can be seen in Fig 1, this includes free space losses, vacuum to glass boundary losses between optical components and diffraction losses. The telescope optics give a gain of 106 dB to compensate for losses over the link distance. A 30 mm beam splitter is attached

to the bottom of the primary mirror to split the optical signal to a Position Sensing Device (PSD) and to an avalanche Photo Diode (APD). The APD is used as the receiver element for communication and has been selected to have an active area diameter of 0.2 mm, with a responsivity of 0.4 A/W at a wavelength of 673 nm (The wavelength of the low power test laser used for evaluation of the engineering model). This will provide a good low cost receiver unit for bench test purposes.
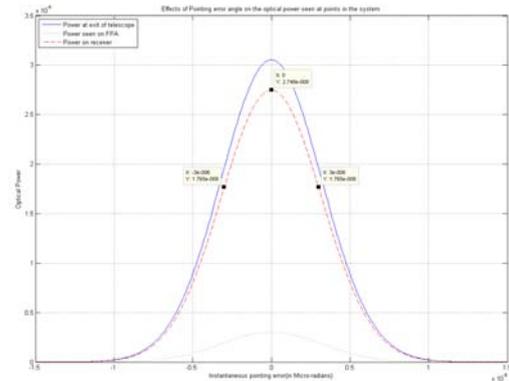

Figure 1. Optical power incident on the receiver as a function of pointing angle over a link distance of 3000km, a laser transmitter of 100 milli-Watts, and a channel bandwidth of 1 gigabit/s, giving a bit error rate (BER) of 10^{-6}. This shows that a pointing error of greater than 3 $\mu rads$ results in a power loss of approximately 40% which results in an unacceptable BER.

The overall dimensions for the engineering model shown in Fig 2 are 240 mm length by 240 mm width with a height of 120 mm to the entrance pupil of the telescope.
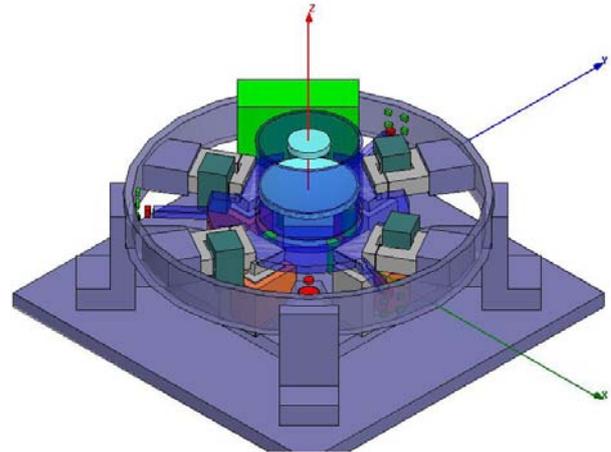

Figure 2. CAD model showing layout of the engineering model being developed for a receiver configuration of the Precise Pointing Mechanism developed in this research for use in optical communications terminals.

The terminal comprises four pairs of permanent magnets (PM's) in a repulsive configuration that have been sized and selected in order to provide a levitation force along the Z axis to provide resistance that opposes the

$$
\begin{bmatrix} F_x \\ F_y \\ F_z \\ T_x \\ T_y \\ T_z \end{bmatrix} = \begin{bmatrix} 0 & 0 & 0 & 0 & k_t & 0 & -k_t & 0 & 0 & 0 & 0 & 0 \\ 0 & 0 & 0 & 0 & 0 & k_t & 0 & -k_t & 0 & 0 & 0 & 0 \\ 1 & 1 & 1 & 1 & 0 & 0 & 0 & 0 & 1 & 1 & 1 & 1 \\ 0 & -r & 0 & r & 0 & 0 & 0 & 0 & r & -r & -r & r \\ -r & 0 & r & 0 & 0 & 0 & 0 & 0 & -r & -r & r & r \\ 0 & 0 & 0 & 0 & rk_t & -rk_t & rk_t & -rk_t & 0 & 0 & 0 & 0 \end{bmatrix} \begin{bmatrix} f_1 \\ f_2 \\ f_3 \\ f_4 \\ f_5 \\ f_6 \\ f_7 \\ f_8 \\ f_9 \\ f_{10} \\ f_{11} \\ f_{12} \end{bmatrix} \quad (1)
$$

reluctance force generated by the four electromagnets controlling the Z displacement and rotations about ϕ and ρ (termed Pointing actuators here after). Permanent magnets are necessary due to the differential requirement when using reluctance force actuators. The forces produced by the pointing actuators for this engineering model total a net force of 12.04 N. The force allows the effects of gravity on the telescope assembly to be offset, as well as providing a force of approximately 0.01 Newtons for the pointing actuators to overcome allowing levitation to be possible. The repulsive forces produced by the permanent magnets is a function of the air gap between the pairs, therefore this is adjustable in order to allow the forces to be tuned on the engineering model leading to a more stable system. The permanent magnets also produce undesired forces that will induce a torque (T_z) about the Z axis, and unwanted translation about X and Y. These are reduced as much as possible through offsetting the mounted position of the permanent magnets so that the net torque and translation is minimized to as close to zero as possible [11]. Through magnetic modeling using the Ansoft Maxwell 3D package the unwanted forces generated were found to be less than 10% of the force produced by the electromagnets when a full $5°$ rotation about ϕ and ρ was commanded, so there is adequate force produced by the electromagnets to overcome these disturbances. In order to levitate the telescope over all 6 DOFs a number of sensors are used to give the position of the telescope. Current contactless sensor technologies allow sensing resolution to the sub-micrometer range (although with a much reduced sensing range). For the purpose of low-cost solution we explore the use of sensing principles that provide uncertainty within ± 100 micrometers but at affordable cost and size. This reasoning is justified by the fact that none of the available sensors can achieve the required $\leq 3\mu$rad resolution, therefore they are used to only levitate the telescope assembly when no optical signal is received. To achieve the required pointing accuracy shown in Fig **??** a PSD is introduced into the optical path which takes a small percentage of the incoming optical signal (focused onto the active area via the telescope), and provides positional information that is mapped in order to calculate the changes required in ϕ and ρ to return the laser spot to the center of the PSD. The center of the PSD corresponds to the center of the APD receiver, therefore maximum power is seen on the APD when the laser spot is in the center of the PSD.

2.2. Terminal Model

The kinematic model of the PPM was derived as Eq. 1. where r is the radius to the electromagnet from the center of the telescope, k_t scales the forces f_5, f_6, f_7, f_8 produced by the translation electromagnets due to the offset rotation of $30°$ (required to allow us to have control over ψ). This kinematic model maps the individual forces produced by the electromagnets to the net forces (F_x, F_y, F_z) and the net torques (T_x, T_y, T_z) about axis X, Y and Z respectively. The repulsive force of the permanent magnets ($f_9, f_{10}, f_{11}, f_{12}$) are modeled using Eq. 2 where K_{pm} is a constant for the force produced by each permanent magnet as a function of surface area (A_{pm}) and the coercive force (H_c), given by $H_c A_{pm}$; ϵ_{pm} is the air gap between the top and bottom permanent magnet.

$$
F_{pm} = \frac{\mu_0 K_{pm1} K_{pm2}}{4\pi \epsilon_{pm}^2} \quad (2)
$$

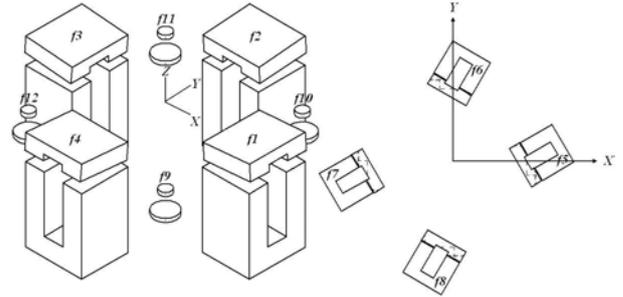The forces acting on the telescope are shown in Fig 3.

Figure 3. Layout showing placement of Electromagnets and forces.

Using this kinematic model the dynamic behavior of the telescope terminal was modeled in the Simulink environment. By applying Newtons second law to the net forces F_x, F_y and F_z it is possible to obtain the translational displacement along the X, Y and Z axis respectively. The inertia of the telescope is given by

Eq. 3.

$$I_T = \begin{bmatrix} 264 & -0.005 & -0.008 \\ -0.008 & 263 & 0.008 \\ 0.008 & -0.005 & 283 \end{bmatrix} e^{-6} kgm^2 \quad (3)$$

The reluctance force (f_n) of each nth electromagnet can be calculated using Eq. 4

$$f_n = -\left(\frac{\mu_o N^2 A_p}{4}\right)\left(\frac{i_n^2}{\epsilon_n^2}\right) \quad (4)$$

where i_n is the current in the nth coil and ϵ_n is the air gap between the rotor and core parts (the rotor being attached to the telescope ring shown in Fig 2), μ_o is the permeability of free-space, N is the number of turns on the electromagnets core and A_p is the area of a single actuator pole face. The force generated by the electromagnets is a reluctance force, therefore the minus sign in Eq. 4 represents the attraction for our model. The sensors are modeled with $\pm$ 100 μmeters random noise to represent the positional accuracy of the sensors used. A simplified diagram representing the principles of the system model can be seen in Fig 4.
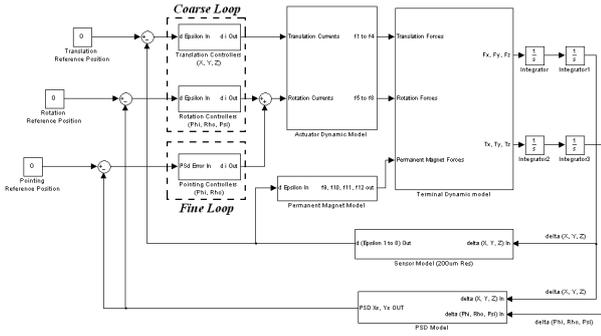

Figure 4. System model of magnetically levitated terminal implemented in Simulink.

2.3. Control system

In order to control the PPM in all 6 DOF a controller for each degree of freedom has been developed. The overall control architecture consists of two control loops. The first loop (termed the coarse loop) controls the levitation of the telescope using only the data from sensors with an accuracy of 200 μmeters. The second loop uses data taken from the PSD that has been transformed to give the required changes in ϕ and ρ. The coarse control loop has been constructed from a Lead-lag compensator. The cut off frequency has been determined from studying the disturbances that affect space craft, and selected to allow the terminal to reject those frequencies of disturbances [4] [5]. In order to derive the controller gain the system is linearized about the operating point. The operating point air gaps are determined by the steady-state air gaps, pointing is 3.7 mm and translation is 0.6 mm. The

operating point currents are determined by the stiffness requirements of the terminal in order to overcome the magnitude of disturbances studied, and in the case of the pointing actuators they need to produce a net force that equals the net force produced by the PM's at steady-state (0.41 A pointing and 0.2 A translation). By applying Taylor series expansion to Eq. 4 and taking only the lower order terms the force from each electromagnet can be represented as Eq. 5.

$$f_n(T) = \frac{\mu_o N^2 A_p i_0^2}{4\epsilon_0^2} + \frac{\mu_o N^2 A_p i_0}{2\epsilon_0^2}\delta i_n - \frac{\mu_o N^2 A_p i_0^2}{2\epsilon_0^3}\delta\epsilon_n$$

$$f_n(T) = f_0 + K_i\delta i_n - K_\epsilon\delta\epsilon_n \quad (5)$$

From Eq. 1 it can be seen that F_x can be simplified to Eq. 6 with the term K_t introduced as gain later in the system.

$$F_x = f_5 - f_7$$

$$F_x = 2K_i\delta i - 2K_\epsilon\delta\epsilon \quad (6)$$

By applying Newtons second law to Eq. 6 we yield

$$F_x = 2K_i\delta i - 2K_\epsilon\delta\epsilon = m_T\ddot{\epsilon}$$

$$G_{(s)} = \frac{\delta\epsilon_n}{\delta i_n} = \frac{\frac{2K_i}{m_T}}{s^2 + \frac{2K_\epsilon}{m_T}} \quad (7)$$

where m_T is the mass of the telescope. A similar approach can be applied to F_y and F_z. By applying Euler's equations of motion to T_x a similar expression for the rotations can be derived. The output from the controllers results in a stable system that is controlled within the 200 μmeters sensor resolution. In a project undertaken in our group, we have demonstrated that commercially available of the shelf (COTS) sensors can achieve a positional accuracy of 2.5 μmeters in translation as shown in Fig 5, and an accuracy of 0.1 milli-radians rotation as seen in Fig 6 [12]. The resolution of the analogue to Digital converters used in Fig 5 is 12bits and the quantization noise present is 1 least significant bit. The ADC to be used in this research is 16bits that will allow a resolution of approximately 0.1 μmeter to be seen. For the design of the fine-pointing loop, the transfer function has been derived numerically for the nonlinear model around the operating point and the system response is depicted in Fig 7. This shows the system has a bandwidth of 128.9 rad/s. This is only one particular case and a higher bandwidth can be achieved by redesigning the coarse-pointing control loop. From Fig 7 it can also be seen that the system has a sensitivity of approximately 1 ampere per millimeter displacement as seen on the PSD. Furthermore, the required pointing sensitivity of 3 μrad will correspond to a change of change of 0.3 mA at steady-state. The fine pointing loop is used to maintain the telescope within 3 $\mu rads$ in order to achieve the designed BER at the set channel bandwidth. This is termed the *fine control loop* and aims to correct for any disturbance in translation or rotation by actively controlling ϕ and ρ to return the laser spot incident on the PSD back to the center of
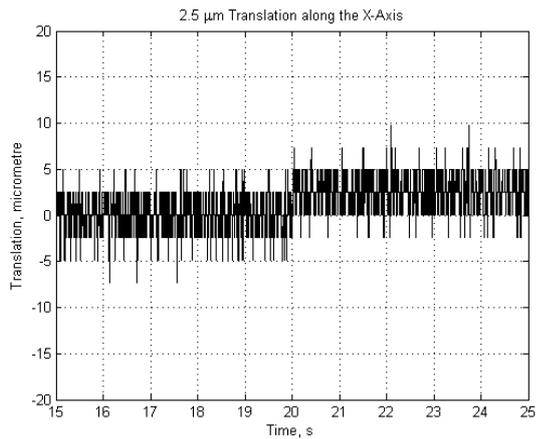
Figure 5. 2.5 μm accuracy as demonstrated by the co-authors.[12].
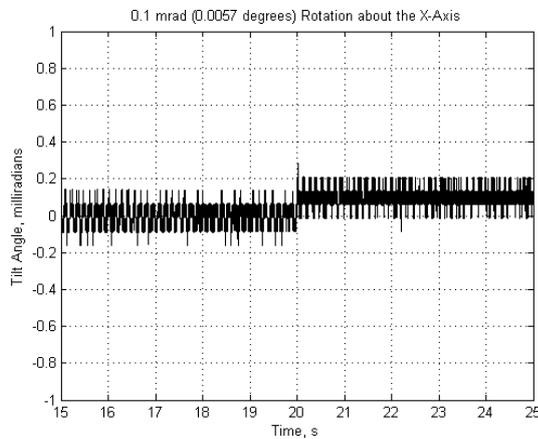

Figure 6. 0.1mrad rotational accuracy of magnetically levitated wheel as demonstrated by the co-authors.[12]

the PSD's active area. This is currently under practical investigation.

3. CONCLUSIONS

An overview, Design and simulation of a 6 DOF magnetically levitated terminal has been discussed here and the design work shown for the coarse control loops. Work is on going to introduce the fine control loop into the system to improve the accuracy of the terminal from the 200 μmeters (due to resolution of low cost COTS sensors) to sub 0.2 μmeters using the PSD data to actively rotate ϕ and ρ in order to overcome translation and pointing positional errors.
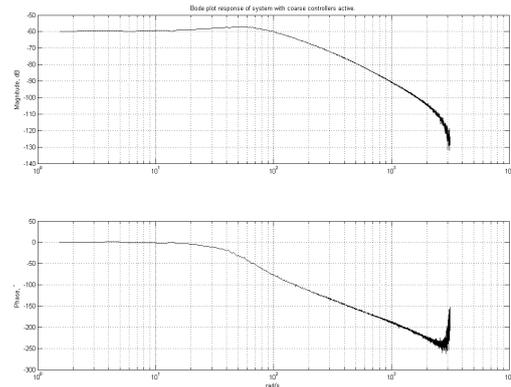

Figure 7. Bode plot response of the system from current demand in the coarse pointing feedback to PSD displacement.

REFERENCES

[1] S.Arnon, S.Rotman and N.S.Kopeika, "Optimum Transmitter Optics Aperture for Satellite Optical communication" IEEE Transactions on Aerospace and Electronic Systems Vol. 43 No.2, April 1998.

[2] G.Baister, P.Gatenby, J.Lewis, M.Wittig, "The SOUT optical Intersatellite communication terminal" IEE proc.-Optoelectron.,Vol.141, No. 6, December 1994.

[3] G.C.Baister, Ch. Haupt, S.Matthews, T.Dreischer, R.Pender and A.Herren,"The ISLFE Terminal Development Project - Results from the Engineering Breadboard Phase", American Institute of Aeronautics and Astronautics 2002.

[4] M Toyoshima amd K Araki, "In-Orbit measurements of short term attitude and vibrational environment on the Engineering Test Satellite VI using laser communication equipment", Society of Optical Photo-Optical Instrumentation Engineers, Opt. Eng. 40, May 2001.

[5] D. C. Bamber, P. Palmer and S. Mackin, "High Performance Attitude Determination through Analysis of Geometric Distortions within Earth Observational Satellite Imagery," Proceedings of the 20th Annual AIAA/USU Conference on Small Satellites, Utah, 2006.

[6] S.Arnon and N.S.Kopeika, "Laser Satellite Communication Network - Vibration Effect and Possible Solutions" Proceedings of the IEEE, Vol. 85, No.10, October 1997.

[7] M. Toyoshima and K Araki, "In-Orbit measurements of the short term attitude and vibrational environment on the Engineering Test Satellite VI using laser communication equipment" Society of Photo-Optical Instrumentation Engineers, 2001.

[8] S Verma, W Kim and J Gu, "Six-Axis Nanopositioning Device with Precision Magnetic Levitation Technology", IEEE/ASME Transactions on Mechatronics, Vol. 9, No. 2, June 2004.

[9] M Y Chen, M J Wang and L C Fu, "Modeling and Controller Design of a Maglev Guiding System for Application in Precision Positioning", IEEE Transactions on Industrial Electronics, Vol. 50, No. 3, June 2003.

[10] Zhaohui Ren and Lyndon Stephens, "Laser Pointing and Tracking using a completely Electromagnetically suspended Actuator", Journal of Guidance, Control and Dynamics, Vol. 29, No. 5, September-October 2006.

[11] S Mukhopashyay, J Donaldson, G Sengupta, S Yamada, C Chakraborty and D Kacprzak, "Fabrication of a Repulsive-Type Magnetic Bearing Using a Novel Arrangement of Permanent Magnets for Vertical-Rotor Suspension.", IEE Transactions on Magnetics, Vol.39, No.5, September 2003.

[12] J Seddon and A Pechev, "3Dwheel: 3-Axis Low Noise, High-Bandwidth Attitude Actuation from a Single Momentum Wheel Using Magnetic Bearings.", 23rd Annual AIAA/USU Conference on Small Satellites, Utah, US, 2009.